BIOCHEMISTRY
including biophysical chemistry & molecular biology

Article

pubs.acs.org/biochemistry

Rapid Exchange of Metal between Zn_7–Metallothionein-3 and Amyloid-β Peptide Promotes Amyloid-Related Structural Changes

Jeppe T. Pedersen,[†,‡,§] Christelle Hureau,[‡] Lars Hemmingsen,[†] Niels H. H. Heegaard,[∥] Jesper Østergaard,[§] Milan Vašák,[⊥] and Peter Faller*[,‡]

[†]Department of Chemistry, Faculty of Science, University of Copenhagen, Universitetsparken 5, DK-2100 Copenhagen, Denmark

[‡]CNRS, LCC (Laboratoire de Chimie de Coordination), 205, route de Narbonne, F-31077 Toulouse, France, and Université de Toulouse, UPS, INPT, LCC, F-31077 Toulouse, France

[§]Department of Pharmaceutics and Analytical Chemistry, Faculty of Pharmaceutical Sciences, University of Copenhagen, Universitetsparken 2, DK-2100 Copenhagen, Denmark

[∥]Department of Clinical Biochemistry and Immunology, Statens Serum Institut, Artillerivej 5, DK-2300 Copenhagen, Denmark

[⊥]Department of Biochemistry, University of Zürich, Winterthurerstrasse 190, 8057 Zurich, Switzerland

Supporting Information

ABSTRACT: Metal ions, especially Zn^{2+} and Cu^{2+}, are implemented in the neuropathogenesis of Alzheimer's disease (AD) by modulating the aggregation of amyloid-β peptides (Aβ). Also, Cu^{2+} may promote AD neurotoxicity through production of reactive oxygen species (ROS). Impaired metal ion homeostasis is most likely the underlying cause of aberrant metal–Aβ interaction. Thus, focusing on the body's natural protective mechanisms is an attractive therapeutic strategy for AD. The metalloprotein metallothionein-3 (MT-3) prevents Cu–Aβ-mediated cytotoxicity by a Zn–Cu exchange that terminates ROS production. Key questions about the metal exchange mechanisms remain unanswered, e.g., whether an Aβ–metal–MT-3 complex is formed. We studied the exchange of metal between Aβ and Zn_7–MT-3 by a combination of spectroscopy (absorption, fluorescence, thioflavin T assay, and nuclear magnetic resonance) and transmission electron microscopy. We found that the metal exchange occurs via free Cu^{2+} and that an Aβ–metal–MT-3 complex is not formed. This means that the metal exchange does not require specific recognition between Aβ and Zn_7–MT-3. Also, we found that the metal exchange caused amyloid-related structural and morphological changes in the resulting Zn–Aβ aggregates. A detailed model of the metal exchange mechanism is presented. This model could potentially be important in developing therapeutics with metal-protein attenuating properties in AD.

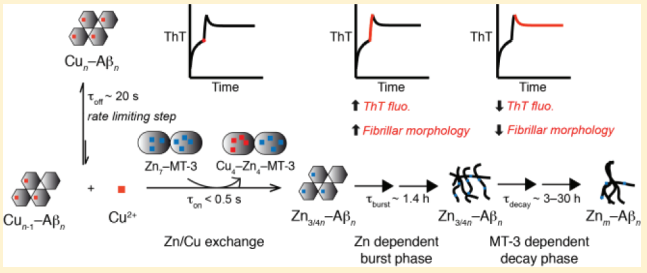

Alzheimer's disease (AD) is a progressive neurodegenerative disease and the most common cause of dementia. Extracellular deposition of cerebral amyloid plaques is a pathological hallmark of AD.[1,2] The plaques mainly consist of amyloid-β peptide ending at residue 40 ($A\beta_{1-40}$) or 42 ($A\beta_{1-42}$). Evidence that metal ions, especially Zn^{2+} and Cu^{2+}, can modulate the aggregation pathways of Aβ upon binding has accumulated.[3−5] For both Cu^{2+} and Zn^{2+}, this occurs immediately (within milliseconds to seconds) upon their binding to Aβ in vitro.[6,7] This suggests that transient synaptic pulses of metal ions reaching micromolar concentrations in the synaptic cleft[8−10] are responsible for deposition of amyloid plaques in vivo.[11]

Interestingly, the roles of Cu^{2+} and Zn^{2+} in AD pathology appear to be distinct; Cu^{2+}-induced Aβ aggregation is associated with neurotoxicity,[12,13] whereas Zn^{2+}-induced aggregation is reported to be neuroprotective or neurotoxic depending on the conditions.[14−17] The differences in neurotoxicity between the Cu^{2+} and Zn^{2+} complexes of Aβ may be related to their difference in production of reactive oxygen species (ROS). While the redox cycling of Cu–Aβ complexes can promote ROS production,[18−21] Zn^{2+} is redox silent.[14] In addition, it has also been suggested that Cu^{2+} promotes Aβ-mediated neurotoxicity by inducing the formation of amyloid fibrils and protofibrils.[13,22] In contrast, Zn^{2+} binding is associated with more amorphous aggregates[6,16] that appear to be less neurotoxic, although toxicity and aggregate structure of Zn–Aβ depend strongly on the conditions used.[23−26] Also, Cu^{2+} has been shown to induce amorphous Aβ aggregates at higher molar Cu^{2+}:Aβ ratios.[5,22,27] Finally, recent evidence suggests a protective role for intracellular Cu in regulating Aβ levels via interference with cell signaling pathways.[28,29]

Received: December 1, 2011
Revised: January 24, 2012
Published: January 28, 2012

Regardless of the exact molecular mechanism of metal-mediated Aβ neurotoxicity, the aberrant metal−Aβ interaction seems to be due to biometal dyshomeostasis in the AD brain.[11,30] Hence, focusing on the endogenous molecules that uphold the metal homeostasis in the body appears to be a feasible therapeutic strategy for preventing Cu−Aβ-mediated neurotoxicity.[31] Specifically, the metalloprotein metallothionein-3 (MT-3) has attracted attention because it is down-regulated in the AD brain[32] and reduces Aβ-mediated cytotoxicity.[33] This infers a neuroprotective role of MT-3 in AD. In the brain, MT-3 is found both in the intra- and extracellular space where it is important in the metal homeostasis of especially Cu^{+} and Zn^{2+}.[34] MT-3 normally binds seven Zn^{2+} ions (termed Zn_7−MT-3) with high affinity ($K_{d,app}$ = 0.16 nM)[35] but can accommodate an additional eighth zinc ion with a lower affinity ($K_{d,app}$ = 100 μM).[36] The seven zinc ions in Zn_7−MT-3 are bound in two metal−thiolate clusters found in two independent domains: the Zn_3−Cys_9 cluster in the N-terminal β-domain (residues 1−32) and the Zn_4−Cys_{11} cluster in the C-terminal α-domain (residues 33−68). It has been shown that exchange of metal ion between Zn_7−MT-3 and Cu−Aβ (both soluble and aggregated) terminates Cu−Aβ-mediated ROS production and significantly decreases cytotoxicity.[37] Recently, a decrease in Cu−Aβ-mediated cytotoxicity was also reported for metallothionein-2 (MT-2).[38] The mode of action of metallothioneins is very particular because it includes both a metal exchange and a reduction of Cu^{2+} to Cu^{+}. This is in contrast to the mode of action of the widely studied metal-protein attenuating compounds (MPACs), which are supposed to bind Cu^{2+} without reduction and metal exchange. Three Zn^{2+} ions from the β-domain in Zn_7−MT-3 are exchanged with four Cu^{2+} ions from Cu−Aβ. After binding to MT-3, Cu^{2+} is reduced by cysteine oxidation, forming redox inert Cu^{I}_4−Zn_4−MT-3.[39] Although it has not been demonstrated, we can assume that binding of Cu^{2+} to cysteines of Zn_7−MT-3 will replace Zn^{2+}, which is then released. Cu^{2+} bound to thiolate will react to form Cu^{+} and a thiyl radical. Upon reaction of a second Cu^{2+} with thiol, the two thiyl radicals form a cysteine disulfide bond. However, key questions about the metal exchange mechanism remain unanswered. Of special interest is whether an Aβ−metal−MT-3 complex is formed during the metal exchange, because formation of ternary ligand−metal−Aβ complexes has been hypothesized to play a role in the actions of the MPACs clioquinol and PBT2.[41] Also, it would be important to determine whether the metal exchange affects the amyloidogenic properties of the Aβ aggregates, because this could offer an alternative mechanism by which MT-3 could modulate Cu−Aβ-mediated neurotoxicity.

In this study, we investigated the mechanism of exchange of metal ions between Zn_7−MT-3 and Cu−$Aβ_{1-40}$ by detailed kinetic spectroscopic methods and transmission electron microscopy. We show that metal ion exchange occurs via free Cu^{2+} on a time scale of seconds to minutes and that metal ion exchange induces time-dependent amyloidogenic structural and morphological changes in $Aβ_{1-40}$ on a time scale of hours. The morphological changes were primarily due to the binding of Zn^{2+} to $Aβ_{1-40}$ aggregates.

MATERIALS AND METHODS

Peptide Preparation and Solubilization. $Aβ_{1-16}$ and $Aβ_{1-40}$ (>96% pure) were synthesized using standard Fmoc chemistry for solid phase peptide synthesis and purchased from Caslo Laboratory. High-performance liquid chromatography indicated a single peak, and the molecular mass was confirmed by ESI-MS. Unless otherwise stated, Aβ stock solutions were prepared by dissolving the peptide in 20 mM HEPES buffer (pH 7.4) containing 100 mM sodium chloride. To minimize the presence of both undissolved Aβ and preformed aggregates,[42] the solution was sonicated for 5 min in an ice bath, centrifuged at 14000*g* for 25 min at 5 °C, and finally filtered (0.22 μm filter). The Aβ concentration was determined using the tyrosine absorbance ($ε_{276}$ = 1410 M^{-1} cm^{-1}). The peptide solutions were used immediately or stored at −20 °C in smaller aliquots for a maximum of 30 days. Prior to use, frozen Aβ was thawed at 5 °C and afterward kept on ice. Before use, the peptide solution was centrifuged at 14000*g* for 25 min[3] at 5 °C immediately after being thawed to remove aggregates. The peptide concentration and pH of the final solution were checked. Differences in the experimental behavior between Aβ that was used immediately and Aβ that had been frozen were not observed.

Recombinant MT-3 was expressed in *Escherichia coli* and purified, as previously described.[43] We used two different types of Zn_7−MT-3 stock solutions: one to which 1 mM dithiothreitol (DTT) was added before stocking and one from which DTT was omitted. In the first type of stock solution, DTT was removed from the Zn_7−MT-3 sample by centrifugation of 2 mL of the sample against 20 mM HEPES buffer (pH 7.4) containing 100 mM sodium chloride using a centricon filter (2 kDa cutoff) at 4000*g* and 5 °C. This procedure was repeated several times by adding more Zn_7−MT-3 solution to increase the concentration of the Zn_7−MT-3 sample. At the end of this procedure, the concentrated Zn_7−MT-3 sample was centrifuged three times with 20 mM HEPES buffer containing 100 mM sodium chloride. The protein concentration, together with the metal and thiolate content, was determined by absorption spectroscopy in 0.1 M HCl ($ε_{220}$ = 53000 M^{-1} cm^{-1}) as previously described[39,43] and used immediately or stored at −20 °C.

Peptide DAHK (Asp-Ala-His-Lys) was purchased from Bachem. Stock solutions were prepared in 20 mM HEPES buffer (pH 7.4) containing 100 mM sodium chloride and stored at −20 °C. Zn^{2+}-loaded DAHK (Zn−DAHK) was prepared prior to being used by addition of 0.8 molar equiv of Zn^{2+}.

The copper stock solution was prepared from $CuCl_2$ in 20 mM HEPES buffer (pH 7.4) containing 100 mM sodium chloride. To prevent precipitation of $Cu(OH)_2$, 4 molar equiv of glycine was added to the stock solutions.[18]

Aggregate Preparation and Isolation. $Aβ_{1-40}$ with and without Cu^{2+} was incubated at 37 °C while being shaken constantly (300 rpm). The samples were centrifuged at 22000*g* and room temperature, and the supernatant was removed. The pellet was resuspended in 20 mM HEPES buffer (pH 7.4) containing 100 mM sodium chloride or 20 mM phosphate with 10% D_2O (pH 7.4) for the nuclear magnetic resonance (NMR) experiments.

ThT Binding Assay. The fibril growth kinetics of $Aβ_{1-40}$ incubated with and without Cu^{2+} was monitored using the amyloid specific dye thioflavin T (ThT). ThT fluorescence was measured using a FLUOstar Optima plate reader system (BMG Labtech) with fluorescence excitation at 440 nm and emission detection at 490 nm. The Aβ concentration was 40 μM and the ThT concentration 20 μM in all experiments. The sample volume was 100 μL, and the plate was incubated at 37 °C. The plate was shaken for 3 s prior to each measurement using a

3 mm orbital shake. Small aliquots of either Zn_7–MT-3, DAHK, Zn–DAHK, or Zn^{2+} were added at different time points. The added volume varied between 1.5 and 2.0 μL depending on the stock concentration of the added species. Thus, the dilution effect was assumed to be negligible.

Absorption Spectroscopy. UV–vis absorption spectra were recorded at 37 °C on a diode array spectrometer (HP 8453 E, Agilent) in a 10 mm path-length quartz cuvette. Absorption spectroscopy at 300 nm was used to monitor the kinetics of binding of Cu^{2+} to Zn_7–MT-3. Cu^{2+} was either free (glycine/buffer complexed) or initially bound to $A\beta_{1-16}$ or $A\beta_{1-40}$. Mixing of species (e.g., $CuCl_2$ and Zn_7–MT-3) was performed in situ by adding one of the species with a pipet to the cuvette containing the other species.

Turbidity. Turbidity was measured at 37 °C using a FLUOstar Optima plate reader system at 350 nm to follow the aggregation kinetics of $A\beta_{1-40}$ (40 μM). The measurement was performed simultaneously with the ThT binding assay using a custom-made script where fluorescence emission was measured followed by turbidity. Zn_7–MT-3, DAHK, Zn–DAHK, and Zn^{2+} were added at different time points (see ThT Binding Assay).

Tyrosine Fluorescence Spectroscopy. Fluorescence spectroscopy was used to monitor the kinetics of dissociation of Cu^{2+} from Cu–$A\beta_{1-16}$ and Cu–$A\beta_{1-40}$ when they were mixed with Zn_7–MT-3. Fluorescence excitation was at 276 nm and emission detection at 315 nm at 37 °C. The procedure for mixing of species (e.g., Cu–$A\beta_{1-16}$ and Zn_7–MT-3) was identical with the one described in Absorption Spectroscopy. Great care was taken to prevent formation of bubbles upon mixing that would otherwise result in light scattering.

NMR Spectroscopy. ^1H NMR spectra were recorded on a Bruker Avance 500 spectrometer equipped with a 5 mm triple-resonance inverse Z-gradient probe. Samples of $A\beta_{1-16}$ (100 μM), freshly prepared $A\beta_{1-40}$ (100 μM), and completely aggregated $A\beta_{1-40}$ were analyzed with and without Zn_7–MT-3 (100 μM). All samples were prepared in 20 mM phosphate with 10% D_2O (pH 7.4).

Transmission Electron Microscopy. Peptide samples were incubated at 37 °C prior to being applied to the grids. Peptide samples (10 μL) were then applied to the grids, washed with Milli-Q water (10 μL), and negatively stained with an aqueous solution of uranyl acetate [10 μL, 1% (w/w)]. Samples were air-dried and examined with a JEOL 1011 transmission electron microscope operating at 100 kV.

Data Analysis. Data analysis and fitting were conducted using the nonlinear least-squares curve fitting program in GraphPad Prism 5.0 (GraphPad Software). UV–vis and tyrosine fluorescence kinetic data were fit to monoexponential or biexponential functions as indicated. ThT fluorescence and turbidity data for apo-$A\beta_{1-40}$ aggregation were fit to a two-step autocatalytic growth model.[44] Here any monomer (M) is irreversibly converted to fibrillar form (F). The fibril can then react with another monomer M as depicted in Scheme 1. The concentration of formed fibrils at time t, $[F]_t$, is mathematically described by

$$[F]_t = [M]_0 - \frac{k_1 + k_2[M]_0}{k_2 + \frac{k_1}{[M]_0}\exp[(k_1 + k_2[M]_0)t]} \quad (1)$$

where $[M]_0$, k_1, and k_2 are the initial monomer concentration, the rate constant of nucleation, and the rate constant of fibril or aggregate growth, respectively. The two reaction steps in Scheme 1 are often composites of many underlying elementary steps. Thus, the rate constants in eq 1 are average rate constants of the underlying steps.[44] The model makes the assumption that the measured experimental signal (e.g., ThT fluorescence intensity) is directly proportional to the mass or concentration of formed fibrils. This was recently verified by comparing the kinetics of fibril formation with the kinetics of soluble peptide loss.[5] Other limitations and assumptions regarding the use of the model are detailed in refs 44 and 45. The burst and decay phases seen in the ThT fluorescence signal for Cu–Aβ upon addition of Zn_7–MT-3 were both fit by a single-exponential function.

Scheme 1. Reaction Mechanism for the Two-Step Autocatalytic Growth Model whereby Monomer M Is Converted to Fibril F[a]

$$M \xrightarrow{k_1} F$$

$$M + F \xrightarrow{k_2} 2F$$

[a]The formed fibril retains its ability to catalyze further fibril formation.

RESULTS AND DISCUSSION

Exchange of Metal between Cu–Aβ and Zn_7–MT-3 Occurs via Free Cu^{2+}. An exchange of metal between Cu^{II}–$A\beta_{1-40}$ and Zn_7^{II}–MT-3 leads to the formation of Zn–$A\beta_{1-40}$ and Cu_4^{I}–Zn_4^{II}–MT-3.[37] However, it has not been reported if the metal exchange occurs via the formation of a ternary complex between Cu^{II}–$A\beta_{1-40}$ and Zn_7^{II}–MT-3 or via free Cu. To address this question, we studied the kinetics and mechanisms of metal exchange by monitoring the transfer of Cu^{2+} from both soluble and aggregated Cu–Aβ to Zn_7–MT-3. $A\beta_{1-16}$ was used as a model for soluble Aβ, because it contains the Cu-binding residues but does not aggregate under the conditions of the experiment. Initially, the rate of binding of Cu^{2+} to Zn_7–MT-3 was investigated by absorption spectroscopy. Binding of Cu^{2+} to Zn_7–MT-3 and subsequent reduction to Cu^+ result in a prominent shoulder at ∼260 mn in the UV–vis absorption spectrum due to the CysS–Cu^I ligand-to-metal charge transfer (LMCT) transition.[46,47] This was also observed in our study (Figure S1 of the Supporting Information). However, the presence of multiple absorbing species around 260 nm impeded specific detection of the binding of Cu to Zn_7–MT-3 at this wavelength. Thus, the kinetics of binding of Cu^{2+} to Zn_7–MT-3 was studied by monitoring the change in absorbance at 300 nm over time. At this wavelength, the CysS–Cu^I absorption bands are less disturbed by other absorbing species; hence, a more selective detection of the Cu–MT-3 complex is possible. A fast increase in absorbance was seen immediately upon mixing of Zn_7–MT-3 with free Cu^{2+} (Figure 1A). The absorbance reached an apparent plateau level after ∼5 s, suggesting that the Cu–Zn–MT-3 complex is rapidly formed (Figure 1A). This is consistent with the previously reported binding of Cu^{2+} to Zn_7–MT-3.[39] The rate-limiting factor could be mixing of Zn_7–MT-3 with Cu^{2+}, because the rate of binding of Cu^{2+} to Zn_7–MT-3 is expected to approach diffusion-limited values.

Next, we followed the exchange of metal between soluble Cu–$A\beta_{1-16}$ and Zn_7–MT-3. As seen from Figure 1B, the apparent rate of binding of Cu^{2+} to Zn_7–MT-3 was slower when Cu^{2+} was initially bound to $A\beta_{1-16}$. This could be explained by assuming that the dissociation of Cu^{2+} from soluble Aβ could be the rate-limiting step, i.e., that binding of Cu^{2+} to Zn_7–MT-3 proceeds via free Cu^{2+}, and not via a

dx.doi.org/10.1021/bi201774z | Biochemistry 2012, 51, 1697–1706

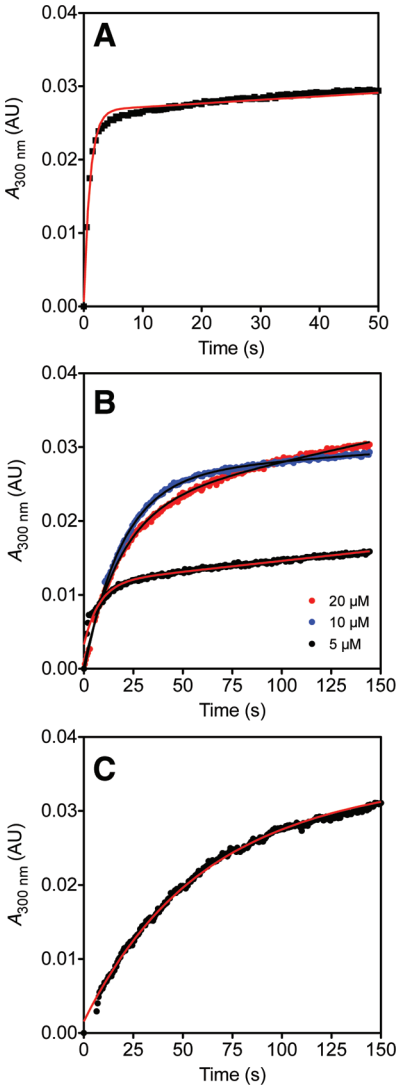

Figure 1. Kinetics of binding of Cu^{2+} to Zn_7–MT-3. (A) Increase in absorption at 300 nm after addition of $CuCl_2$ (20 μM) to Zn_7–MT-3 (10 μM). (B) Increase in absorption at 300 nm after addition of Cu–Aβ_{1-16} (20 and 40 μM) to Zn_7–MT-3 (5, 10, and 20 μM). (C) Increase in absorption at 300 nm after addition of Cu–Aβ_{1-40} aggregates (20 and 40 μM) to Zn_7–MT-3 (10 μM). Solid lines are fits to a single-exponential function. Experiments were performed in 20 mM HEPES and 100 mM NaCl (pH 7.4) at 37 °C.

transient Aβ–Cu–Zn_7–MT-3 complex. To test this hypothesis, we investigated the relationship between Zn_7–MT-3 concentration and the rate of Cu^{2+} binding (Figure 1B). The rate of binding of Cu^{2+} to Zn_7–MT-3 did not increase with an increase in Zn_7–MT-3 concentration. This supports the finding that dissociation of Cu^{2+} from Aβ_{1-16} is the rate-limiting step in the metal exchange reaction. In addition, the apparent rate constant of 0.08 ± 0.02 s^{-1} [total mean for all three concentration levels ± the standard error of the mean (SEM)] for Cu^{2+} binding is similar to the determined k_{off} of 0.10 s^{-1} for the dissociation of Cu^{2+} from Aβ_{1-16} under identical experimental conditions (temperature, pH, and buffer).[7] This further supports the finding that dissociation of Cu^{2+} from Aβ_{1-16} is the rate-limiting step in the reaction of Cu^{2+}–Aβ_{1-16} with Zn_7–MT-3. Note that the final absorption value increases with an increase in Zn_7–MT-3 concentration (Figure 1B), although MT-3 is fully copper-loaded even at 5 μM. The reason for this increase is most likely interference from multiple absorbing species as in the case at 260 nm (see above), and secondary (slower) processes in connection with binding of Cu to MT-3. However, this does not influence our analysis of the initial kinetics of binding of Cu to MT-3. We further note that the absorption measurements of the Cu^{2+} binding kinetics are not perturbed by Zn^{2+}-induced aggregation of Aβ, because this would lead to an increase in apparent absorbance due to light scattering. Light scattering increases with lower wavelengths, which is not observed (Figure S1A of the Supporting Information).

Hereafter, we studied the exchange of metal between Cu–Aβ_{1-40} aggregates and Zn_7–MT-3 (Figure 1C). We found an apparent rate constant of 0.03 ± 0.01 s^{-1} for the binding of aggregate-bound Cu^{2+} to Zn_7–MT-3. This rate constant also agrees well with the k_{off} determined for Cu–Aβ_{1-40} (0.052 s^{-1}).[7] This indicates that dissociation of Cu^{2+} is also rate-limiting in the exchange of metal between Zn_7–MT-3 and Aβ_{1-40} aggregates.

Taken together, our data imply that the binding kinetics is controlled by the rate of dissociation of Cu^{2+} from Cu–Aβ. This indicates that the transfer of Cu from Aβ to Zn_7–MT-3 proceeds via free Cu^{2+} for both monomeric and aggregated Cu–Aβ.

Chemical shifts of the resonances were not observed in ^{1}H NMR experiments upon mixing of Zn_7–MT-3 and Aβ_{1-16}. Moreover, addition of preaggregated Aβ_{1-40} did not induce chemical shifts in the resonances of Zn_7–MT-3. Hence, indications of a complex between Zn_7–MT-3 and Aβ were not found. This supports the notion that an Aβ–metal–MT-3 complex is not involved in metal exchange. Note that experiments cannot be conducted in the presence of Cu^{2+}, as Cu^{2+} broadens the Aβ signals beyond detection and a change in the resonances of MT-3 is expected due to Cu^{2+} binding and reduction.

Metal Exchange Induces Changes in the Tyrosine Fluorescence of Aβ_{1-16}. Binding of Cu^{2+} to Aβ induces structural changes in the Tyr10 environment in Aβ that allows characterization of the binding kinetics. In the presence of Cu^{2+}, the fluorescence intensity of Tyr10 in Aβ_{1-16} was immediately partially quenched because of Cu^{2+} binding as previously reported[48] (Figure 2, inset). When Zn_7–MT-3 was added to Cu–Aβ_{1-16}, the fluorescence intensity rapidly increased (Figure 2).

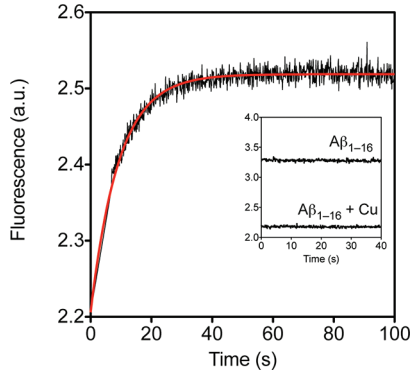

Figure 2. Tyrosine fluorescence of Cu–Aβ_{1-16} (20 and 40 μM) after addition of Zn_7–MT-3 (10 μM). Fluorescence data were fit (red trace) to a monoexponential function. The inset shows tyrosine fluorescence of Aβ_{1-16} (40 μM) and Cu–Aβ_{1-16} (20 and 40 μM). Experiments were performed in 20 mM HEPES and 100 mM NaCl (pH 7.4) at 37 °C.

The increase in fluorescence occurred on the same time scale (0–25 s) that was seen for the increase in absorbance (Figure 1B). An apparent rate constant (k_{app}) of 0.108 ± 0.001 s^{-1}

dx.doi.org/10.1021/bi201774z | Biochemistry 2012, 51, 1697–1706

(best fit parameter ± SEM) was determined for the increase in fluorescence intensity. This is similar to the apparent rate constant determined in the absorption experiment. This confirms that the metal exchange rate is limited by the dissociation of Cu^{2+} from $A\beta_{1-16}$.

Next we investigated the change in tyrosine fluorescence intensity of aggregated Cu−$A\beta_{1-40}$ upon addition of Zn_7−MT-3. Zn_7−MT-3 also caused an increase in the tyrosine fluorescence of $A\beta_{1-40}$ aggregates. However, the interpretation of data is confounded by the light scattering due to aggregated $A\beta_{1-40}$, which may perturb the fluorescence measurements.[7] Therefore, additional measurements were undertaken to verify whether structural changes in $A\beta$ occurred.

Exchange of Metal between Zn_7−MT-3 and Cu−$A\beta$ Induces Amyloid-Related Changes. We studied the effect of Zn_7−MT-3 on the amyloidogenicity and aggregation kinetics of $A\beta_{1-40}$ and Cu−$A\beta_{1-40}$ by monitoring the ThT fluorescence and turbidity. Zn_7−MT-3 was added at different time points along the aggregation pathway of apo- and holo-$A\beta_{1-40}$ to test whether the amyloidogenic state of the $A\beta$ oligomers is important for Zn_7−MT-3-induced structural changes.[37]

First, we investigated the influence of Zn_7−MT-3 (10 μM) on the fibrillation of apo-$A\beta_{1-40}$ (40 μM). Zn_7−MT-3 did not affect either the ThT fluorescence or the turbidity time profiles of $A\beta_{1-40}$ (Figure S2 of the Supporting Information). This supports the findings of the ^{1}H NMR experiments. Both the ThT and turbidity time profiles of apo-$A\beta_{1-40}$ had a sigmoid curve shape, which is characteristic of a nucleation phase followed by elongation and a plateau phase.

Addition of Cu^{2+} to $A\beta_{1-40}$ caused a rapid increase in both ThT fluorescence and turbidity (Figure 3A,B, blue traces) as previously reported.[5] The increases in ThT fluorescence and turbidity indicate that Cu^{2+} induced formation of amyloidogenic aggregates and oligomers.

Hereafter, we studied the influence of Zn_7−MT-3 on the Cu^{2+}-induced aggregation of $A\beta_{1-40}$. Zn_7−MT-3 (10 μM) was added immediately after the addition of Cu^{2+} (20 μM) to $A\beta_{1-40}$ (40 μM), or after incubation with Cu^{2+} for 15, 23, and 46 h. Zn_7−MT-3 induced a fast exponential increase (burst) in the ThT fluorescence intensity of Cu−$A\beta_{1-40}$ irrespective of the time of addition. The rapid increase in ThT fluorescence reached a maximum after ~2.5−3 h, followed by a slow exponential decay in intensity (Figure 3A). In contrast, the turbidity was not affected by addition of Zn_7−MT-3 after prolonged incubation with Cu^{2+} (Figure 3B). This indicates that the metal exchange does not significantly influence the mean size of the Cu−$A\beta_{1-40}$ aggregates. However, when Zn_7−MT-3 is added immediately after addition of Cu^{2+}, there appears to be a second lag phase from 7 to 16 h (Figure 3B, black circles). This lag phase may be caused by the rapid removal of Cu^{2+} from $A\beta$ by Zn_7−MT-3 before all the peptide becomes aggregated.

The initial increase in ThT fluorescence is most likely connected to the exchange of Cu and Zn between Cu−$A\beta$ and Zn_7−MT-3, because Zn_7−MT-3 did not affect the ThT fluorescence of apo-$A\beta$ (vide supra). Interestingly, the Zn_7−MT-3-induced increase in ThT fluorescence occurs on a time scale much longer than those of both the increase in absorbance at 300 nm, which reflects the binding of Cu^{2+} to MT-3 (Figure 1), and the increase in tyrosine fluorescence intensity, which reflects the dissociation of Cu^{2+} from $A\beta$ (Figure 2). The initial increases in ThT fluorescence intensity (burst phase) at the different time points were fit to monoexponential functions with almost identical rate constants (k_{burst}) of ~2 × 10^{-4} s^{-1} (Table 1). Hence, the increase in ThT fluorescence intensity is ~100 times slower than the increase in absorbance at 300 nm and tyrosine fluorescence intensity; i.e., the amyloid-related structural changes of the $A\beta$ aggregates occur after the transfer of Cu^{2+} between $A\beta$ and MT-3 has taken place. This suggests that the amyloid-related changes are not due to dissociation of Cu from Cu−$A\beta$ aggregates, but rather due to Zn^{2+} binding.

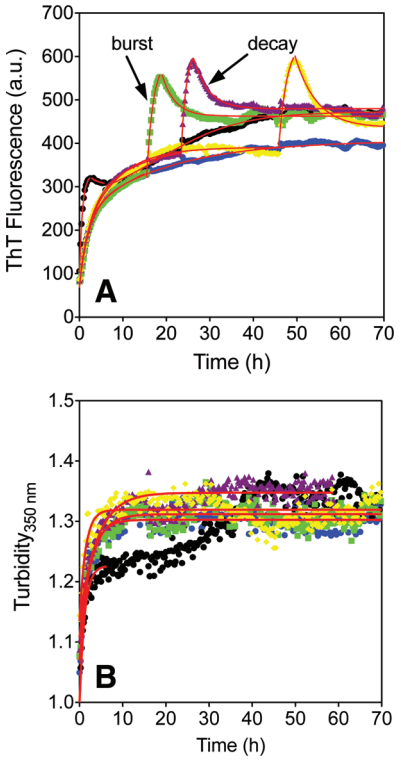

Figure 3. Influence of Zn_7−MT-3 on the fibrillation of Cu−$A\beta_{1-40}$. (A) ThT fluorescence and (B) turbidity (λ = 350 nm) of Cu−$A\beta_{1-40}$ (20 and 40 μM) upon addition of Zn_7−MT-3 (10 μM) at various times after incubation with Cu: 0 (●), 15 (green squares), 23 (purple triangles), and 46 h (yellow diamonds). Fluorescence time profiles for Cu−$A\beta_{1-40}$ without addition of Zn_7−MT-3 are also shown (blue circles). The presented time profiles are an average of a minimum of three traces. The burst and decay phase in panel A are fit to monoexponentials. Experiments were performed in 20 mM HEPES and 100 mM NaCl (pH 7.4) at 37 °C.

To investigate this, we studied how Zn^{2+}, the model peptide DAHK, and Zn−DAHK affected the ThT fluorescence of Cu−$A\beta$. DAHK is a stronger Cu^{2+} chelator than $A\beta$ and is able to extract Cu^{2+} from soluble and aggregated $A\beta$.[49,50] Addition of apo-DAHK to Cu−$A\beta_{1-40}$ did not affect the ThT fluorescence (Figure 4, inset). This supports the conclusion that the increase in ThT fluorescence is not due to removal of Cu. In contrast, addition of Zn^{2+}−DAHK or Zn^{2+} caused an increase in ThT fluorescence intensity (Figure 4) similar to the Zn_7−MT-3-induced increase in ThT fluorescence. This supports the idea that the amyloid-related changes in $A\beta$ are caused by Zn^{2+} binding and is consistent with observations that Zn−$A\beta$ emits a stronger ThT signal than apo-$A\beta$.[23] Moreover, the Zn^{2+}-induced increase in the ThT fluorescence intensity of $A\beta$ agrees with findings that Zn^{2+} promotes the β-sheet conformation of $A\beta$[51,52] whereas Cu^{2+} does not.[48,53] Note, however, that contradicting results with respect to Zn^{2+} exist on this subject.[54,55] Finally, the Zn^{2+}-induced increase in ThT fluorescence intensity indicates that removal of Cu^{2+} is not necessary for binding of Zn^{2+} to Cu−$A\beta$.

dx.doi.org/10.1021/bi201774z | Biochemistry 2012, 51, 1697−1706

Table 1. Apparent Rate Constants for the Increase in the Level of ThT Positive Aggregates for the Aggregation of Cu−Aβ_{1-40} (20 and 40 μM) upon Addition of Zn_7−MT-3 (10 μM) at Different Times (t_{add})[a]

system	plateau ThT intensity	k_{burst} ($\times 10^{-4}$ s^{-1})	k_{decay} ($\times 10^{-4}$ s^{-1})
Cu−Aβ_{1-40} without Zn_7−MT-3	407 ± 1	–	–
Cu−Aβ_{1-40} with Zn_7−MT-3 (t_{add} = 0)	473 ± 9	4.0 ± 0.2	not determined
Cu−Aβ_{1-40} with Zn_7−MT-3 (t_{add} = 15 h)	463 ± 1	1.8 ± 0.4	0.94 ± 0.08
Cu−Aβ_{1-40} with Zn_7−MT-3 (t_{add} = 23 h)	480 ± 1	2.5 ± 0.6	0.82 ± 0.07
Cu−Aβ_{1-40} with Zn_7−MT-3 (t_{add} = 46 h)	438 ± 2	1.5 ± 0.1	0.56 ± 0.05

[a] k_{burst} is the rate constant for the exponential increase in ThT fluorescence, while k_{decay} is the rate constant for the exponential decrease in ThT fluorescence (Figure 3A). Parameters for the rate constants are best fitted values ± SEM. Experiments were performed in 20 mM HEPES and 100 mM NaCl (pH 7.4) at 37 °C.

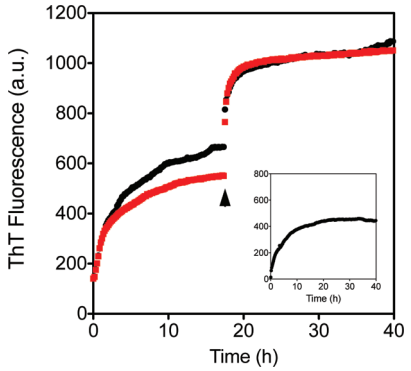

Figure 4. ThT fluorescence of Cu−Aβ (40 and 40 μM) upon addition of Zn^{2+} (30 μM) (●) or Zn−DAHK (30 and 40 μM) (red squares) after 17 h. The inset shows the ThT fluorescence of Cu−Aβ (20 and 40 μM) upon addition of DAHK (40 μM) after 3 h. Experiments were performed in 20 mM HEPES and 100 mM NaCl (pH 7.4) at 37 °C.

This is consistent with recent studies showing that Aβ_{1-16} can simultaneously bind Zn^{2+} and Cu^{2+},[56,57] and that Zn^{2+} does dot replace Cu^{2+} in Cu−Aβ_{1-16}.[57] Further note that the conditional K_d (i.e., the apparent binding constant at pH 7.4 in the absence of competing buffer) of Aβ_{1-40} for Cu^{2+} is in the picomolar to nanomolar range[42,58,59] while it is in the micromolar range for Zn^{2+}.[26,59]

Contrary to the experiments with Zn_7−MT-3, the Zn^{2+}- and Zn−DAHK-induced increases in ThT fluorescence were not followed by a decrease in ThT fluorescence. Thus, it seems that this decay in ThT fluorescence is specific to MT-3. The origin of the decay in ThT fluorescence is not known but could reflect further rearrangement of the amyloids or a re-uptake of Zn^{2+} from Zn−Aβ by MT-3, and the possibility that (weak) interactions between aggregated Zn−Aβ and Cu_4−Zn_4−MT-3 are taking place cannot be excluded.

Exchange of Metal between MT-3 and Aβ Causes Changes in Aggregate Morphology. The MT-3-induced increase in ThT fluorescence indicates that binding of Zn^{2+} to Aβ shifts the Cu−Aβ aggregates toward a more fibrillar morphology and/or exposes more ThT binding sites, which may otherwise be inaccessible in the Cu−Aβ aggregates. We therefore studied morphological changes in Cu−Aβ aggregates induced by the metal exchange using TEM (i) at the maximum of the ThT fluorescence burst (~3 h after addition of Zn_7−MT-3) and (ii) at the end of the ThT decay phase (>15 h after addition of Zn_7−MT-3). Incubation of Aβ_{1-40} with Cu^{2+} rapidly produced small amorphous aggregates with little or no fibrillar structure as previously reported[5,27,49] (Figure 5A and Figure S3 of the Supporting Information). Next, Zn_7−MT-3 was added to fully aggregated Cu−Aβ_{1-40} (incubated for 72 h). Three hours after the addition of Zn_7−MT-3, the morphology of the aggregates had changed from amorphous aggregates into more fibrillar structures (Figure 5B and Figure S3 of the Supporting Information). This change in morphology could explain the observed increase in ThT fluorescence,

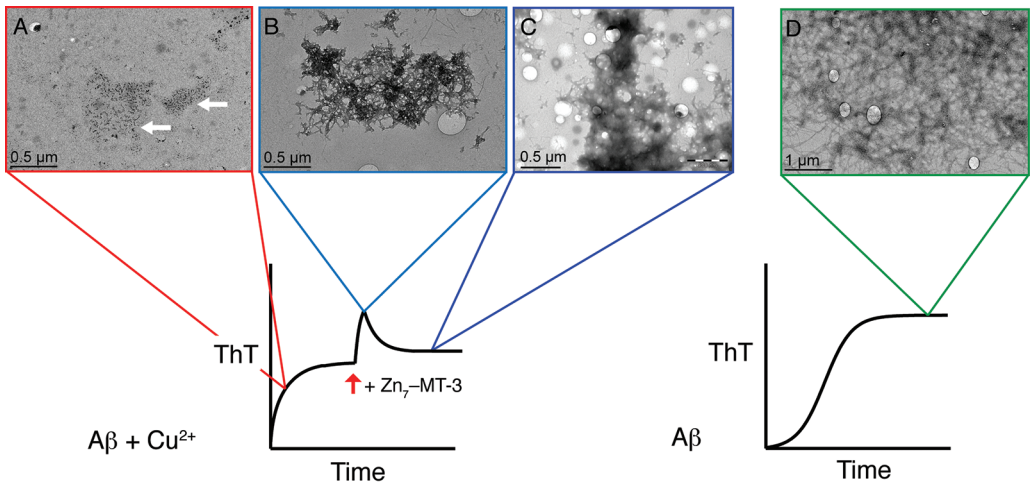

Figure 5. TEM images of (A) Cu−Aβ_{1-40} (20 and 40 μM) analyzed after incubation for 20 min; the arrows indicate Cu^{2+}-induced aggregates. (B) Cu−Aβ_{1-40} (20 and 40 μM) with addition of Zn_7−MT-3 (10 μM) after 72 h and analyzed after 75 h (3 h after addition of Zn_7−MT-3). (C) Cu−Aβ_{1-40} (20 and 40 μM) with addition of Zn_7−MT-3 (10 μM) after 72 h and analyzed after 88 h (16 h after addition of Zn_7−MT-3). (D) Aβ_{1-40} (40 μM) incubated for 72 h. A schematic presentation of the corresponding ThT curve based upon Figure 3A and Figure S2 of the Supporting Information is shown. Experiments were performed in 20 mM HEPES and 100 mM NaCl (pH 7.4) at 37 °C.

dx.doi.org/10.1021/bi201774z | Biochemistry 2012, 51, 1697−1706

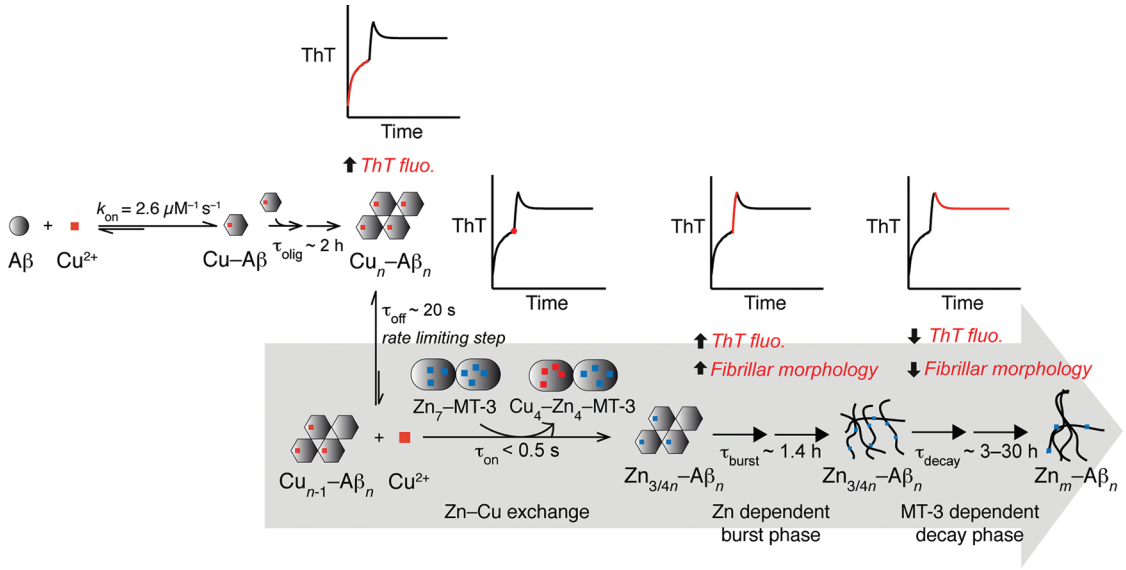

Figure 6. Proposed mechanism for exchange of metal between Cu−Aβ_{1-40} and Zn_7−MT-3. In the top panel, Cu^{2+} induces formation of ThT positive Aβ aggregates. In the bottom panel, Zn_7−MT-3 binds free Cu^{2+} dissociated from the Cu−Aβ complex. The exchange of Zn^{2+} for Cu^{2+} causes a rapid increase in ThT fluorescence, and a concurrent shift in the morphology of the Aβ aggregates from amorphous to fibrillar. A slow decrease in ThT fluorescence is observed in parallel with morphological changes on a longer time scale. The decrease in ThT fluorescence appears to be dependent on MT-3. Not all reactions are explicitly shown. The large gray arrow indicates the overall direction of the reactions. The rate constant, k_{on}, for initial binding of Cu^{2+} to Aβ was taken from ref 7. The time constant ($\tau = 1/k$) for dissociation of Cu^{2+} from Aβ (τ_{off}) was determined from ref 7. Other time constants (τ_{on}, τ_{burst}, and τ_{decay}) were determined from rate constants in this study.

because fibrils are expected to produce a stronger ThT signal than amorphous aggregates.[60] The morphology of the Aβ aggregates seen at the maximum of the ThT burst resembles the morphology of Aβ aggregates incubated with Zn^{2+}.[23] This suggests that it is primarily the binding of Zn^{2+} released from Zn_7−MT-3 that is responsible for these initial morphological changes.

At 16 h upon addition of Zn_7−MT-3 (Figure 5C and Figure S3 of the Supporting Information), fibrils that more resembled the fibrils seen for apo-Aβ incubated with Zn_7−MT-3 were observed.[23] The fibrillar structures seen in the decay phase of the ThT fluorescence appear to be more clustered together than those observed after 3 h (the ThT maximum). This could explain the decrease in ThT fluorescence following the initial rapid increase. However, more studies are needed to understand the molecular mechanism of this decay. It should be noted that fibrillar aggregates seen upon addition of Zn_7−MT-3 to Cu−Aβ are different from the fibrils seen for apo-Aβ (Figure 5D).

Taken together, the TEM data support the observations by ThT fluorescence; amorphous Cu−Aβ aggregates are observed prior to the ThT fluorescence burst (Figure 5A) followed by a shift toward more fibrillar structures after a few hours [maximal ThT fluorescence burst (Figure 5B)]. Finally an apparent decrease in the number of fibrillar structures is observed after the decay of the ThT fluorescence signal has been completed (Figure 5C).

In this study, we used a combination of kinetic spectroscopic methods (ThT assay, absorption, and fluorescence spectroscopy), electron microscopy, and NMR spectroscopy to explore the mechanism of the exchange of metal ion between Cu−Aβ and Zn_7−MT-3. The results are compatible with the mechanistic model of metal exchange presented in Figure 6. The observed kinetic results strongly suggest that the transfer of Cu^{2+} from Cu−Aβ to Zn_7−MT-3 proceeds via free Cu^{2+}, and that the neuroprotective exchange of metal between Cu−Aβ and Zn_7−MT-3 does not involve an Aβ−Cu−MT-3 complex. This is interesting because the intermolecular exchange of Cu^{2+} between Aβ occurs via a ternary Aβ−Cu−Aβ complex,[7] and exchange of zinc from MT-2 has previously been indicated to occur via a ternary ligand−Zn−MT-2 complex.[61] Also, our findings that an Aβ−Cu−MT-3 complex is not formed during metal exchange imply that MT-3-mimicking drugs do not necessarily need specific recognition by Aβ. (It is clear that recognition of Aβ by drugs acting on the amyloid cascade Aβ, including MPACs, can be very important in targeting the drug to its place of action and/or if they have also an anti-aggregation activity, but for the removal or exchange of metal itself, it is not crucial.) This could be important in therapeutic applications.

The aggregation mechanism and aggregation states of Aβ and Cu−Aβ have been linked to cellular toxicity.[13,27] Thus, the amyloid-related structural (ThT data) and morphological (TEM data) changes of Aβ aggregates induced by MT-3 may be related to the protective role of Zn_7−MT-3 against Cu−Aβ-mediated toxicity. In addition, it has recently been suggested that the release of Zn^{2+} from Zn_7−MT3 and subsequent binding to Aβ and the ability of MTs to redistribute zinc could also be important in neuroprotection.[23,62] However, the relevance of the Zn^{2+}/Zn_7−MT-3 induced structural changes in Aβ to any neuroprotective effect cannot be determined from our data.

In summary, our study shows that Zn_7−MT-3 induces structural and morphological changes in Cu−Aβ. This is consistent with previous findings[23,37,38] and clearly underlines the difference between the mode of action of Zn_7−MT-3 and that of compounds that only withdraw Cu^{2+} from Cu−Aβ (like DAHK) and hence do not induce such structural and morphological changes in Cu−Aβ under the conditions described here. Moreover, our study indicates that the aggregational behavior and structure of Cu−Aβ can be modulated by the presence of other species released in the

dx.doi.org/10.1021/bi201774z | Biochemistry 2012, 51, 1697−1706

synaptic cleft, e.g., MT-3 and Zn^{2+}. Thus, multiple factors may affect Aβ aggregation and the structure of amyloid aggregates in vivo. This needs to be considered when designing metal-targeting drugs for AD based on the metal exchange mechanism of MT-3.

■ ASSOCIATED CONTENT

Supporting Information

UV−vis spectra of (A) Cu−Aβ_{1-16} and (B) aggregated Cu−Aβ_{1-40} (Figure S1), influence of Zn_7−MT-3 on the fibrillation of apo-Aβ_{1-40} monitored by (A) ThT fluorescence and (B) turbidity (Figure S2), and additional TEM images of the influence of Zn_7−MT-3 on Cu^{2+}-induced Aβ aggregates (Figure S3). This material is available free of charge via the Internet at http://pubs.acs.org.

■ AUTHOR INFORMATION

Corresponding Author

*E-mail: peter.faller@lcc-toulouse.fr. Telephone: +33(0)5 61 33 31 62.

Funding

This work is supported by funding from Statens Serum Institut, the Drug Research Academy, Faculty of Pharmaceutical Sciences, University of Copenhagen, and The Villum Kann Rasmussen Foundation and from the "Region Midi-Pyrénées" (Grant APRTCN09004783).

Notes

The authors declare no competing financial interest.

■ ACKNOWLEDGMENTS

Vincent Colliere (LCC, Toulouse, France) is thanked for performing transition electron microscopy measurements. Christian Bijani (LCC, Toulouse, France) is thanked for performing NMR spectroscopy.

■ ABBREVIATIONS

AD, Alzheimer's disease; Aβ, amyloid-β; DTT, dithiothreitol; F, fibrillar form of peptide; HEPES, 4-(2-hydroxyethyl)-1-piperazineethanesulfonic acid; LMCT, ligand-to-metal charge transfer; MPAC, metal-protein attenuating compound; M, monomer form; MT-2, metallothionein-2; MT-3, metallothionein-3; ROS, reactive oxygen species; TEM, transmission electron microscopy; ThT, thioflavin t; τ, time constant; Zn_7−MT-3, Zn_7−metallothionein-3.

■ REFERENCES

(1) Hardy, J., and Selkoe, D. J. (2002) The amyloid hypothesis of Alzheimer's disease: Progress and problems on the road to therapeutics. *Science 297*, 353−356.

(2) Roychaudhuri, R., Yang, M., Hoshi, M. M., and Teplow, D. B. (2009) Amyloid β-protein assembly and Alzheimer disease. *J. Biol. Chem. 284*, 4749−4753.

(3) Atwood, C. S., Moir, R. D., Huang, X. D., Scarpa, R. C., Bacarra, N. M. E., Romano, D. M., Hartshorn, M. K., Tanzi, R. E., and Bush, A. I. (1998) Dramatic aggregation of Alzheimer Aβ by Cu(II) is induced by conditions representing physiological acidosis. *J. Biol. Chem. 273*, 12817−12826.

(4) Bush, A. I., Pettingell, W. H., Multhaup, G., Paradis, M. D., Vonsattel, J. P., Gusella, J. F., Beyreuther, K., Masters, C. L., and Tanzi, R. E. (1994) Rapid induction of Alzheimer Aβ amyloid formation by zinc. *Science 265*, 1464−1467.

(5) Pedersen, J. T., Østergaard, J., Rozlosnik, N., Gammelgaard, B., and Heegaard, N. H. H. (2011) Cu(II) mediates kinetically distinct, non-amyloidogenic aggregation of amyloid-β peptides. *J. Biol. Chem. 286*, 26952−26963.

(6) Noy, D., Solomonov, I., Sinkevich, O., Arad, T., Kjaer, K., and Sagi, I. (2008) Zinc-amyloid β interactions on a millisecond time-scale stabilize non-fibrillar Alzheimer-related species. *J. Am. Chem. Soc. 130*, 1376−1383.

(7) Pedersen, J. T., Teilum, K., Heegaard, N. H. H., Østergaard, J., Adolph, H. W., and Hemmingsen, L. (2011) Rapid formation of a preoligomeric peptide−metal−peptide complex following copper(II) binding to amyloid β peptides. *Angew. Chem., Int. Ed. 50*, 2532−2535.

(8) Kardos, J., Kovács, I., Hajós, F., Kálmán, M., and Simonyi, M. (1989) Nerve endings from rat brain tissue release copper upon depolarization. A possible role in regulating neuronal excitability. *Neurosci. Lett. 103*, 139−144.

(9) Hopt, A., Korte, S., Fink, H., Panne, U., Niessner, R., Jahn, R., Kretzschmar, H., and Herms, J. (2003) Methods for studying synaptosomal copper release. *J. Neurosci. Methods 128*, 159−172.

(10) Li, Y., Hough, C. J., Suh, S. W., Sarvey, J. M., and Frederickson, C. J. (2001) Rapid translocation of Zn^{2+} from presynaptic terminals into postsynaptic hippocampal neurons after physiological stimulation. *J. Neurophysiol. 86*, 2597−2604.

(11) Barnham, K. J., and Bush, A. I. (2008) Metals in Alzheimer's and Parkinson's diseases. *Curr. Opin. Chem. Biol. 12*, 222−228.

(12) Huang, X., Cuajungco, M. P., Atwood, C. S., Hartshorn, M. A., Tyndall, J. D., Hanson, G. R., Stokes, K. C., Leopold, M., Multhaup, G., Goldstein, L. E., Scarpa, R. C., Saunders, A. J., Lim, J., Moir, R. D., Glabe, C., Bowden, E. F., Masters, C. L., Fairlie, D. P., Tanzi, R. E., and Bush, A. I. (1999) Cu(II) potentiation of Alzheimer Aβ neurotoxicity. Correlation with cell-free hydrogen peroxide production and metal reduction. *J. Biol. Chem. 274*, 37111−37116.

(13) Sarell, C. J., Wilkinson, S. R., and Viles, J. H. (2010) Substoichiometric levels of Cu^{2+} ions accelerate the kinetics of fiber formation and promote cell toxicity of amyloid-β from Alzheimer disease. *J. Biol. Chem. 285*, 41533−41540.

(14) Cuajungco, M. P., Goldstein, L. E., Nunomura, A., Smith, M. A., Lim, J. T., Atwood, C. S., Huang, X., Farrag, Y. W., Perry, G., and Bush, A. I. (2000) Evidence that the β-amyloid plaques of Alzheimer's disease represent the redox-silencing and entombment of Aβ by zinc. *J. Biol. Chem. 275*, 19439−19442.

(15) Cardoso, S. M., Rego, A. C., Pereira, C., and Oliveira, C. R. (2005) Protective effect of zinc on amyloid-β 25−35 and 1−40 mediated toxicity. *Neurotoxic. Res. 7*, 273−281.

(16) Garai, K., Sahoo, B., Kaushalya, S. K., Desai, R., and Maiti, S. (2007) Zinc lowers amyloid-β toxicity by selectively precipitating aggregation intermediates. *Biochemistry 46*, 10655−10663.

(17) Ryu, J., Girigoswami, K., Ha, C., Ku, S. H., and Park, C. B. (2008) Influence of multiple metal ions on β-amyloid aggregation and dissociation on a solid surface. *Biochemistry 47*, 5328−5335.

(18) Huang, X. D., Atwood, C. S., Hartshorn, M. A., Multhaup, G., Goldstein, L. E., Scarpa, R. C., Cuajungco, M. P., Gray, D. N., Lim, J., Moir, R. D., Tanzi, R. E., and Bush, A. I. (1999) The Aβ peptide of Alzheimer's disease directly produces hydrogen peroxide through metal ion reduction. *Biochemistry 38*, 7609−7616.

(19) Opazo, C., Huang, X., Cherny, R. A., Moir, R. D., Roher, A. E., White, A. R., Cappai, R., Masters, C. L., Tanzi, R. E., Inestrosa, N. C., and Bush, A. I. (2002) Metalloenzyme-like activity of Alzheimer's disease β-amyloid. Cu-dependent catalytic conversion of dopamine, cholesterol, and biological reducing agents to neurotoxic H_2O_2. *J. Biol. Chem. 277*, 40302−40308.

(20) Hureau, C., and Faller, P. (2009) Aβ-mediated ROS production by Cu ions: Structural insights, mechanisms and relevance to Alzheimer's disease. *Biochimie 91*, 1212−1217.

(21) Balland, V., Hureau, C., and Savéant, J. M. (2010) Electrochemical and homogeneous electron transfers to the Alzheimer amyloid-β copper complex follow a preorganization mechanism. *Proc. Natl. Acad. Sci. U.S.A. 107*, 17113−17118.

(22) Jun, S. M., and Saxena, S. (2007) The aggregated state of amyloid-β peptide in vitro depends on Cu^{2+} ion concentration. *Angew. Chem., Int. Ed. 46*, 3959−3961.

(23) Durand, J., Meloni, G., Talmard, C., Vašák, M., and Faller, P. (2010) Zinc release of Zn_7-metallothionein-3 induces fibrillar type amyloid-β aggregates. *Metallomics 2*, 741−744.
(24) Kodali, R., Williams, A. D., Chemuru, S., and Wetzel, R. (2010) Aβ(1−40) forms five distinct amyloid structures whose β-sheet contents and fibril stabilities are correlated. *J. Mol. Biol. 401*, 503−517.
(25) Cuajungco, M. P., and Fagét, K. Y. (2003) Zinc takes the center stage: Its paradoxical role in Alzheimer's disease. *Brain Res. Rev. 41*, 44−56.
(26) Tõugu, V., Tiiman, A., and Palumaa, P. (2011) Interactions of Zn(II) and Cu(II) ions with Alzheimer's amyloid-β peptide. Metal ion binding, contribution to fibrillization and toxicity. *Metallomics 3*, 250−261.
(27) Smith, D. P., Ciccotosto, G. D., Tew, D. J., Fodero-Tavoletti, M. T., Johanssen, T., Masters, C. L., Barnham, K. J., and Cappai, R. (2007) Concentration dependent Cu^{2+} induced aggregation and dityrosine formation of the Alzheimer's disease amyloid-β peptide. *Biochemistry 46*, 2881−2891.
(28) Donnelly, P. S., Caragounis, A., Du, T., Laughton, K. M., Volitakis, I., Cherny, R. A., Sharples, R. A., Hill, A. F., Li, Q. X., and Masters, C. L. (2008) Selective intracellular release of copper and zinc ions from bis(thiosemicarbazonato) complexes reduces levels of Alzheimer disease amyloid-β peptide. *J. Biol. Chem. 283*, 4568−4577.
(29) Crouch, P. J., Hung, L. W., Adlard, P. A., Cortes, M., Lal, V., Filiz, G., Perez, K. A., Nurjono, M., Caragounis, A., and Du, T. (2009) Increasing Cu bioavailability inhibits Aβ oligomers and tau phosphorylation. *Proc. Natl. Acad. Sci. U.S.A. 106*, 381−386.
(30) Zatta, P., Drago, D., Bolognin, S., and Sensi, S. L. (2009) Alzheimer's disease, metal ions and metal homeostatic therapy. *Trends Pharmacol. Sci. 30*, 346−355.
(31) Duce, J. A., and Bush, A. I. (2010) Biological metals and Alzheimer's disease: Implications for therapeutics and diagnostics. *Prog. Neurobiol. 92*, 1−18.
(32) Yu, W. H., Lukiw, W. J., Bergeron, C., Niznik, H. B., and Fraser, P. E. (2001) Metallothionein III is reduced in Alzheimer's disease. *Brain Res. 894*, 37−45.
(33) Irie, Y., and Keung, W. M. (2001) Metallothionein-III antagonizes the neurotoxic and neurotrophic effects of amyloid β peptides. *Biochem. Biophys. Res. Commun. 282*, 416−420.
(34) Vašák, M., and Hasler, D. W. (2000) Metallothioneins: New functional and structural insights. *Curr. Opin. Chem. Biol. 4*, 177−183.
(35) Hasler, D. W., Jensen, L. T., Zerbe, O., Winge, D. R., and Vašák, M. (2000) Effect of the two conserved prolines of human growth inhibitory factor (metallothionein-3) on its biological activity and structure fluctuation: Comparison with a mutant protein. *Biochemistry 39*, 14567−14575.
(36) Meloni, G., Polanski, T., Braun, O., and Vašák, M. (2009) Effects of Zn^{2+}, Ca^{2+}, and Mg^{2+} on the structure of Zn_7metallothionein-3: Evidence for an additional zinc binding site. *Biochemistry 48*, 5700−5707.
(37) Meloni, G., Sonois, V., Delaine, T., Guilloreau, L., Gillet, A., Teissié, J., Faller, P., and Vašák, M. (2008) Metal swap between Zn7-metallothionein-3 and amyloid-β-Cu protects against amyloid-β toxicity. *Nat. Chem. Biol. 4*, 366−372.
(38) Chung, R. S., Howells, C., Eaton, E. D., Shabala, L., Zovo, K., Palumaa, P., Sillard, R., Woodhouse, A., Bennett, W. R., Ray, S., Vickers, J. C., and West, A. K. (2010) The native copper- and zinc-binding protein metallothionein blocks copper-mediated Aβ aggregation and toxicity in rat cortical neurons. *PLoS One 5*, e12030.
(39) Meloni, G., Faller, P., and Vašák, M. (2007) Redox silencing of copper in metal-linked neurodegenerative disorders: Reaction of Zn_7metallothionein-3 with Cu^{2+} ions. *J. Biol. Chem. 282*, 16068−16078.
(40) Rigo, A., Corazza, A., di Paolo, M. L., Rossetto, M., Ugolini, R., and Scarpa, M. (2004) Interaction of copper with cysteine: Stability of cuprous complexes and catalytic role of cupric ions in anaerobic thiol oxidation. *J. Inorg. Biochem. 98*, 1495−1501.
(41) Bush, A. I., and Tanzi, R. E. (2008) Therapeutics for Alzheimer's disease based on the metal hypothesis. *Neurotherapeutics 5*, 421−432.
(42) Hatcher, L. Q., Hong, L., Bush, W. D., Carducci, T., and Simon, J. D. (2008) Quantification of the binding constant of copper(II) to the amyloid-β peptide. *J. Phys. Chem. B 112*, 8160−8164.
(43) Faller, P., Hasler, D. W., Zerbe, O., Klauser, S., Winge, D. R., and Vašák, M. (1999) Evidence for a dynamic structure of human neuronal growth inhibitory factor and for major rearrangements of its metal-thiolate clusters. *Biochemistry 38*, 10158−10167.
(44) Morris, A. M., Watzky, M. A., Agar, J. N., and Finke, R. G. (2008) Fitting neurological protein aggregation kinetic data via a 2-step, minimal/"Ockham's Razor" model: The Finke-Watzky mechanism of nucleation followed by autocatalytic surface growth. *Biochemistry 47*, 2413−2427.
(45) Morris, A. M., Watzky, M. A., and Finke, R. G. (2009) Protein aggregation kinetics, mechanism, and curve-fitting: A review of the literature. *Biochim. Biophys. Acta 1794*, 375−397.
(46) Pountney, D. L., Schauwecker, I., Zarn, J., and Vašák, M. (1994) Formation of mammalian Cu_8-metallothionein in vitro: Evidence for the existence of two $Cu(I)_4$-thiolate clusters. *Biochemistry 33*, 9699−9705.
(47) Roschitzki, B., and Vašák, M. (2002) A distinct Cu_4-thiolate cluster of human metallothionein-3 is located in the N-terminal domain. *J. Biol. Inorg. Chem. 7*, 611−616.
(48) Syme, C. D., Nadal, R. C., Rigby, S. E. J., and Viles, J. H. (2004) Copper binding to the amyloid-β (Aβ) peptide associated with Alzheimer's disease: Folding, coordination geometry, pH dependence, stoichiometry, and affinity of Aβ-(1−28): Insights from a range of complementary spectroscopic techniques. *J. Biol. Chem. 279*, 18169−18177.
(49) Perrone, L., Mothes, E., Vignes, M., Mockel, A., Figueroa, C., Miquel, M. C., Maddelein, M. L., and Faller, P. (2010) Copper transfer from Cu-Aβ to human serum albumin inhibits aggregation, radical production and reduces Aβ toxicity. *ChemBioChem 11*, 110−118.
(50) Trapaidze, A., Hureau, C., Bal, W., Winterhalter, M., and Faller, P. (2012) Thermodynamic study of Cu^{2+} binding to the DAHK and GHK peptides by isothermal titration calorimetry (ITC) with the weaker competitor glycine. *J. Biol. Inorg. Chem. 17*, 37−47.
(51) Yang, D. S., McLaurin, J., Qin, K., Westaway, D., and Fraser, P. E. (2000) Examining the zinc binding site of the amyloid-β peptide. *Eur. J. Biochem. 267*, 6692−6698.
(52) Mancino, A. M., Hindo, S. S., Kochi, A., and Lim, M. H. (2009) Effects of clioquinol on metal-triggered amyloid-β aggregation revisited. *Inorg. Chem. 48*, 9596−9598.
(53) Brzyska, M., Trzesniewska, K., Wieckowska, A., Szczepankiewicz, A., and Elbaum, D. (2009) Electrochemical and conformational consequences of copper (Cu(I) and Cu(II)) binding to β-amyloid(1−40). *ChemBioChem 10*, 1045−1055.
(54) Yoshiike, Y., Tanemura, K., Murayama, O., Akagi, T., Murayama, M., Sato, S., Sun, X. Y., Tanaka, N., and Takashima, A. (2001) New insights on how metals disrupt amyloid β-aggregation and their effects on amyloid-β cytotoxicity. *J. Biol. Chem. 276*, 32293−32299.
(55) Raman, B., Ban, T., Yamaguchi, K., Sakai, M., Kawai, T., Naiki, H., and Goto, Y. (2005) Metal ion-dependent effects of clioquinol on the fibril growth of an amyloid β peptide. *J. Biol. Chem. 280*, 16157−16162.
(56) Damante, C. A., Ösz, K., Nagy, Z., Grasso, G., Pappalardo, G., Rizzarelli, E., and Sóvágó, I. (2011) Zn^{2+}'s Ability to Alter the Distribution of Cu^{2+} among the Available Binding Sites of Aβ(1−16)-Polyethylenglycolylated Peptide: Implications in Alzheimer's Disease. *Inorg. Chem. 50*, 5342−5350.
(57) Liu, L., and Xia, N. (2012) Zinc-mediated modulation of the configuration and activity of complexes between copper and amyloid-β peptides. *Biochem. Biophys. Res. Commun. 417*, 153−156.
(58) Rózga, M., Kłoniecki, M., Dadlez, M., and Bal, W. (2010) A direct determination of the dissociation constant for the Cu(II) complex of amyloid β 1−40 peptide. *Chem. Res. Toxicol. 23*, 336−340.
(59) Faller, P., and Hureau, C. (2009) Bioinorganic chemistry of copper and zinc ions coordinated to amyloid-β peptide. *Dalton Trans. 7*, 1080−1094.

(60) Groenning, M. (2010) Binding mode of Thioflavin T and other molecular probes in the context of amyloid fibrils: Current status. *J. Chem. Biol. 3*, 1−18.
(61) Jacob, C., Maret, W., and Vallee, B. L. (1998) Control of zinc transfer between thionein, metallothionein, and zinc proteins. *Proc. Natl. Acad. Sci. U.S.A. 95*, 3489−3494.
(62) Bell, S. G., and Vallee, B. L. (2009) The metallothionein/thionein system: An oxidoreductive metabolic zinc link. *ChemBioChem 10*, 55−62.